NUMERICAL SIMULATION OF DROP IN A CONSTRICTED MICRO-CAPILLARY USING FINITE ELEMENT AND LEVEL SET METHODS

Jose F. Roca, jfrr2030@yahoo.com
Marcio S. Carvalho, msc@puc-rio.br
Department of Mechanical Engineering, Pontificia Universidade Catolica do Rio de Janeiro (PUC-RIO), Rua Marques de Sao Vicente 225, Gavea, RJ, 22453-900, Brazil

Abstract. *The study of drop dynamics through straight and constricted capillaries has been carried out. Finite element and level set methods are used in order to get the behavior of pressure gradient as a function of imposed flow rate, capillary geometry, drop size, viscosity ratio of drop and continuous phase and capillary number. The Navier-Stokes and level set equations are used to solve two-phase immiscible flow. These equations are solved by using Petrov-Galerkin method. However, the level set method has disadvantages such as loss of mass conservation and thick interface thickness. To avoid this, special techniques should be considered in the formulation such as reinitialization of the scalar function among others. Numerical results are obtained by using our FEM program developed in FORTRAN and compared with available experimental data.*

Keywords:*Finite element method, level set method, constricted micro-capillary.*

1. INTRODUCTION

The injection of oil-water emulsions through porous media as an enhanced oil recovery method has attracted an important interest. As it was stated by McAuliffe (1973), the rapid channeling of water from injection zones through high permeability reservoir areas gives low oil recovery. Thus, when oil-in-water emulsions are injected, emulsion enters these high permeability zones and its dispersed phase restricts the flow, so water starts to flow into low permeability zones improving sweep efficiency. Hence this method may decrease the permeability of swept zones by blocking pores.

Many experimental studies have been carried out in order to understand the blocking mechanism, for example the study of the flow of a single drop immersed in a continuous phase through a capillary conducted by Ho and Leal (1975) and Olbricht and Leal (1982). They noted that extra pressure drop in the capillary depends on ratio between drop and capillary diameters, viscosity ratio and flow rate. Recently, Cobos *et al.* (2009) analyzed the problem also experimentally and reported how pressure varied due to the presence of the drop in the constricted capillary, explaining one of the blocking mechanism.

This particular study aims to understand the phenomena by modeling and simulating the drop dynamics through a constricted capillary due to imposed flow rate.

Shen and Udell (1985) used finite element methods to solve a semi-infinite bubble flowing in a cylindrical straight tube, in their work the shape of the bubble menisci was located by balancing surface tension forces against viscous and pressure forces, the effect of capillary number on the drop shape and flow field was also studied. Tsai and Miksis (1994) carried out the dynamics model of a drop in a constricted and straight capillaries by using a boundary integral method, they also examined snap-off process. Despite the fact that, there are many approaches to solve liquid-liquid interface problems, such as moving grid formulation, also called Langranian approach, the fixed grid formulation or Eulerian approach is explored in this study, particularly the level set method.

In his Ph.D. thesis, Sussman (1994) developed an approach for computing the interface of two immiscible fluids, by using level set method, the interface is captured instead of being tracked. Unlike the moving grid method, the fixed grid formulation is easier to implement and to generalize to 3D problems. However, there are serious drawbacks related to mass conservation and interface thickness. Sussman *et al.* (1995) also reported the simulation of air-water flow handling large density ratios, as well as surface tension and viscosity effects. Osher and Sethian (1988) developed new algorithms to approximate equations of propagating fronts, which are Hamilton-Jacobi equations with viscosity terms and solved many surface problems. Tryggvason *et al.* (2001) discussed the wide variety of methods for computing multiphase flows, classifying in four types, they also presented their method as a hybrid between a front capturing and a front-tracking approach, which uses a stationary grid for the fluid flow as a whole whilst the interface is tracked by another grid.

On the other hand, it should be noted that modeling the surface force is challenging, Shepel and Smith (2008) modeled the surface tension force as a distributed body force concentrated in a band near the interface. They discussed two methods, the first models the interface by using a delta function, and in the second the force not only acts near the interface, it is also in the cells which the interface is contained.

2. FORMULATION

The flow is sketched in Fig. 1. The problem is governed by the Navier-Stokes equations for unsteady, viscous, Newtonian, incompressible two-phase flow. The model is simplified as an axisymmetrical problem, neglecting the density difference between both fluids and gravity effects.

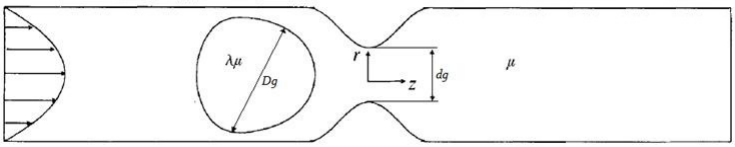

Figure 1. Drop in a constricted capillary, Tsai and Miksis (1994)

The governing equations for conservation of mass and momentum are,

$$\rho\frac{\partial\bar{u}}{\partial t}+\rho\bar{u}.\bar{\nabla}\bar{u}=\bar{\nabla}.\bar{\bar{T}}+\rho\bar{f} \tag{1}$$

$$\frac{\partial\rho}{\partial t}+\bar{\nabla}.\rho\bar{u}=0 \tag{2}$$

where ρ is the density, $\bar{u}$ is the velocity vector field, $\bar{\bar{T}}$ is the stress tensor, $\bar{f}$ is the body force.

In addition, for a Newtonian model fluid is known,

$$\bar{\bar{T}}=-p\bar{\bar{I}}+\mu[\bar{\nabla}\bar{u}+\bar{\nabla}\bar{u}^{T}] \tag{3}$$

where p is the pressure scalar field and μ is the viscosity defined as,

$$\mu(c)=\mu_1+(\mu_2-\mu_1)H\varepsilon(c) \tag{4}$$

where μ_1 and μ_2 are viscosities of oil and water respectively and $H\varepsilon(c)$ (see Fig. 2) known as smoothed Heaviside function is given by,

$$H\varepsilon(c)=\frac{c+\varepsilon}{2\varepsilon}+\frac{1}{2\pi}\sin(\frac{\pi c}{\varepsilon}) \tag{5}$$

which is a continuous function that helps to improve the numerical stability when the viscosity is interpolated across the interface and depends on a scalar field c that defines each liquid phase. The evolution of the scalar function is described by the following advection equation,

$$\frac{\partial c}{\partial t}+\bar{u}.\bar{\nabla}c=0 \tag{6}$$

where c captures the liquid-liquid interface.

Traditionally, c is defined as a signed distance function measured from the interface to any position. However, c can also be defined as a marker function which assigns -1 to the drop domain Ω_1 and $+1$ to the capillary domain Ω_2.

3. NUMERICAL METHOD

In this section, the Navier-Stokes and level set equations are solved by using the Petrov-Galerkin finite element formulation. Furthermore, this study is not only intended to solve velocity and pressure fields as well as the scalar field c which defines the liquid-liquid interface.

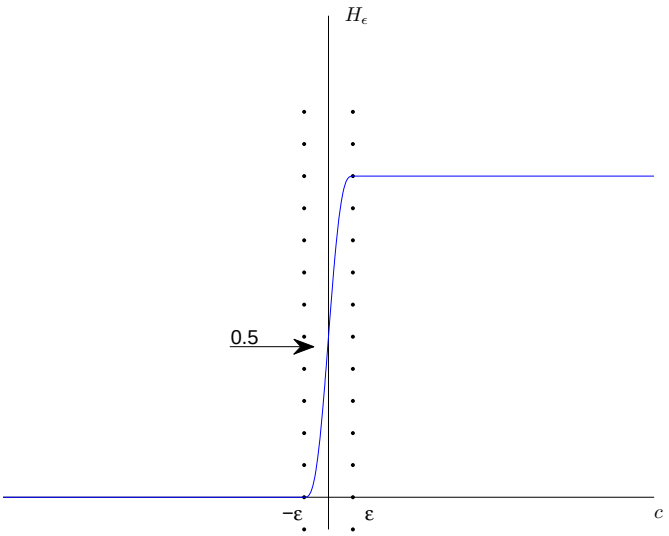

Figure 2. Smoothed Heaviside function

The weak formulations of Eq. (1), Eq. (2) considering incompressible fluids and Eq. (6) are given by,

$$R_m = \int_\Omega (\rho \frac{\partial \bar{u}}{\partial t} + \rho \bar{u}.\bar{\nabla}\bar{u} - \bar{\nabla}.\bar{\bar{T}} - \rho \bar{f}).W \, d\Omega \tag{7}$$

$$R_{mc} = \int_\Omega (\bar{\nabla}.\bar{u})\chi \, d\Omega \tag{8}$$

$$R_c = \int_\Omega (\frac{\partial c}{\partial t} + \bar{u}.\bar{\nabla}c)\psi \, d\Omega \tag{9}$$

where W, χ and ψ are weighting functions of momentum, continuity and level set equations respectively. Notice the weighting function W is a vector function.

After manipulations, considering both fluids as Newtonian and taking into consideration the cylindrical coordinates r and z, the residuals are described as,

$$\begin{aligned} R^i_{mr} &= \int_\Omega \rho \frac{\partial v_r}{\partial t}\phi_i \, d\Omega + \int_\Omega \rho(v_z \frac{\partial v_r}{\partial z} + v_r \frac{\partial v_r}{\partial r})\phi_i \, d\Omega \\ &+ \int_\Omega \{\mu(\frac{\partial v_r}{\partial z} + \frac{\partial v_z}{\partial r})\frac{d\phi_i}{dz} + (-p + 2\mu \frac{\partial v_r}{\partial r})\frac{d\phi_i}{dr} + \frac{1}{r}(-p + 2\mu \frac{v_r}{r})\phi_i\} \, d\Omega \\ &- \int_\Gamma f_r \phi_i \, d\Gamma - \int_\Omega \rho f^B_r \phi_i \, d\Omega; i = 1, \cdots, n \end{aligned} \tag{10}$$

$$\begin{aligned} R^i_{mz} &= \int_\Omega \rho \frac{\partial v_z}{\partial t}\phi_i \, d\Omega + \int_\Omega \rho(v_z \frac{\partial v_z}{\partial z} + v_r \frac{\partial v_z}{\partial r})\phi_i \, d\Omega \\ &+ \int_\Omega \{(-p + 2\mu \frac{\partial v_z}{\partial z})\frac{d\phi_i}{dz} + \mu(\frac{\partial v_r}{\partial z} + \frac{\partial v_z}{\partial r})\frac{d\phi_i}{dr}\} \, d\Omega \\ &- \int_\Gamma f_z \phi_i \, d\Gamma - \int_\Omega \rho f^B_z \phi_i \, d\Omega; i = 1, \cdots, n \end{aligned} \tag{11}$$

$$R^i_{mc} = \int_\Omega (\frac{\partial v_z}{\partial z} + \frac{\partial v_r}{\partial r} + \frac{v_r}{r})\chi_i \, d\Omega; i = 1, \cdots, m \tag{12}$$

$$R^i_c = \int_\Omega \frac{\partial c}{\partial t}\psi_i \, d\Omega + \int_\Omega (v_z \frac{\partial c}{\partial z} + v_r \frac{\partial c}{\partial r})\psi_i \, d\Omega; i = 1, \cdots, n \tag{13}$$

where v_r and v_z are velocity components, f_r and f_z are boundary forces components, f_r^B and f_z^B are body forces components and finally n and m are numbers of degrees of freedom of velocity and pressure respectively.

The velocity vector field $\bar{v}$ and the scalar field c are expanded in terms of bi-quadratic lagrangian functions and the pressure field p by piece-wise linear discontinuous functions χ_i. Relating to weighting functions, Garlerkin formulation in Eq. (7) describes weighting function equals to basis functions, whereas the Petrov-Galerkin formulation defines weighting function ψ_i used in Eq. (13) as,

$$\psi_i = \phi_i + h\frac{\bar{u}}{\|\bar{u}\|}.\bar{\nabla}\phi_i \tag{14}$$

where h is a parameter used in Stream Upwind Petrov-Galerkin (SUPG) formulations to stabilize the method.

It should be mentioned that the above equations are arranged in the following vector known as residual vector,

$$\mathbf{R} = \begin{pmatrix} R^i_{mr} \\ R^i_{mz} \\ R^i_c \\ R^i_{mc} \end{pmatrix} \tag{15}$$

Hence the solution vector is defined as,

$$\mathbf{S_V} = \begin{pmatrix} V_{rj} \\ V_{zj} \\ C_j \\ P_j \end{pmatrix} \tag{16}$$

Then the jacobian matrix is defined as,

$$\mathbf{J} = \frac{\partial \mathbf{R}}{\partial \mathbf{S_V}} \tag{17}$$

and expanded as follows,

$$\mathbf{J} = \begin{pmatrix} \frac{\partial R^i_{mr}}{\partial V_{rj}} & \frac{\partial R^i_{mr}}{\partial V_{zj}} & \frac{\partial R^i_{mr}}{\partial C_j} & \frac{\partial R^i_{mr}}{\partial P_j} \\ \frac{\partial R^i_{mz}}{\partial V_{rj}} & \frac{\partial R^i_{mz}}{\partial V_{zj}} & \frac{\partial R^i_{mz}}{\partial C_j} & \frac{\partial R^i_{mz}}{\partial P_j} \\ \frac{\partial R^i_c}{\partial V_{rj}} & \frac{\partial R^i_c}{\partial V_{zj}} & \frac{\partial R^i_c}{\partial C_j} & \frac{\partial R^i_c}{\partial P_j} \\ \frac{\partial R^i_{mc}}{\partial V_{rj}} & \frac{\partial R^i_{mc}}{\partial V_{zj}} & \frac{\partial R^i_{mc}}{\partial C_j} & \frac{\partial R^i_{mc}}{\partial P_j} \end{pmatrix} \tag{18}$$

The numerical integrations were performed with nine-point Gauss quadrature. Furthermore, the nonlinear problem is addressed by using the Newton method, which solves a linear system of equations at every step until convergence is reached,

$$\mathbf{J}\Delta{\mathbf{S_V}}^{k+1} = -\mathbf{R}({\mathbf{S_V}}^k) \tag{19}$$

with,

$${\mathbf{S_V}}^{k+1} = {\mathbf{S_V}}^k + \Delta{\mathbf{S_V}}^{k+1} \tag{20}$$

The initial guess for the next time step is obtained with a first order approximation which estimates the next value by considering present and previous values and given here by,

$$\mathbf{S_V}_{i+1} - \mathbf{S_V}_i = \frac{\mathbf{S_V}_i - \mathbf{S_V}_{i-1}}{t_i - t_{i-1}}(t_{i+1} - t_i) \tag{21}$$

where $i-1$, i and $i+1$ are previous, present and the next steps of time respectively.

4. NUMERICAL RESULTS

Numerical results were obtained by using our FEM program developed in FORTRAN, simulated in a Windows™ operating system and run in a Dell™ Vostro™ 200 computer.

In this study, we used the flow rate as an input data and the pressure gradient is obtained numerically. Moreover, three capillaries of different geometries such as $100\mu m$, $100/50\mu m$ and $200/50\mu m$ were modeled. At this stage, we simulate only a drop geometry and a viscosity ratio, without considering surface tension effects.

Figure 3 shows for didactic purpose a grid obtained by our FEM software. Notice that the constricted region has more elements in order to get a better resolution.

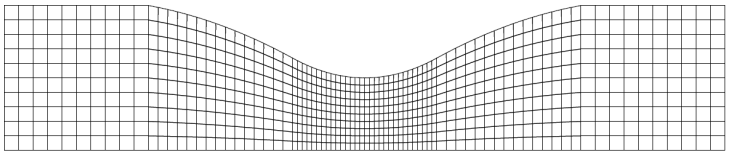

Figure 3. Example of a fixed grid in a $100/50\mu$m constricted capillary

Figure 4 depicts the pressure drop with respect to flow rate for a single phase flow through straight and constricted capillaries. As we can see, there is a larger pressure gradient when a constricted capillary is used. This is consistent with the experimental results of Robles and Carvalho (2010).

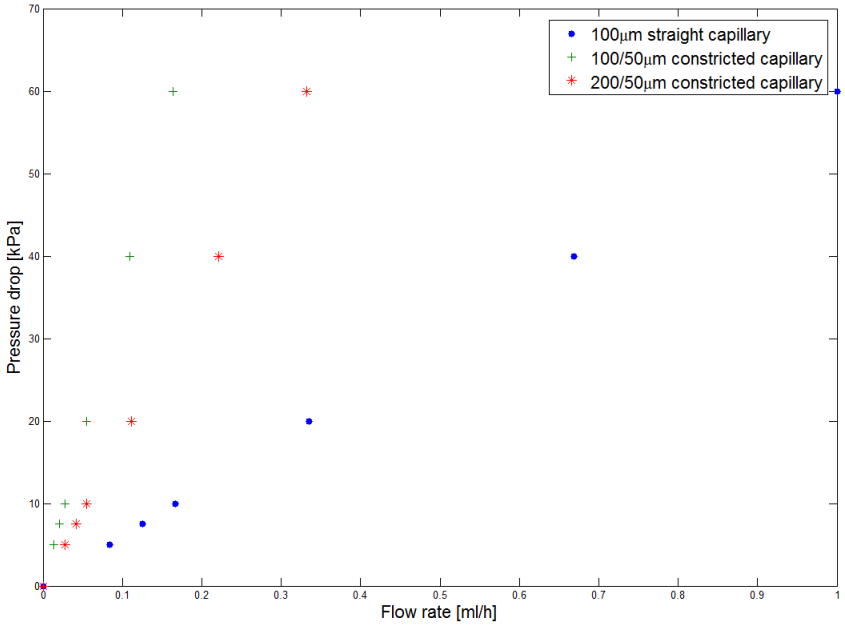

Figure 4. Pressure drop with respect to flow rate in three capillaries

4.1 Straight capillary

As it was mentioned before c is a marker function which assigns to the drop domain the value -1 and the continuous phase $+1$. In addition, some simulation parameters such as $\Delta t = 0.001s$, $t_f = 0.15s$, input flow rate $Q = 0.07ml/h$, output pressure $P_{OUT} = 0kPa$, $\rho = 1000kg/m^3$, μ_1=0.11 Pa.s and μ_2=0.22 Pa.s were considered initially.

In Fig. 5 the evolution of a 60μm drop initially spherical through the 100μm straight capillary due to an imposed flow rate is plotted, as we can see the drop practically vanishes.

$$V_{DROP} = 2\pi \int_{\Omega} H\varepsilon(-c)\, d\Omega \tag{22}$$

The volume evolution of the same drop is observed in Fig. 6 by using Eq. (22), and so is depicted how loss of mass drop evolves with respect to time and we see that the curve slope is steep, for this reason the drop disappears rapidly. Sussman (1994) and other researchers reported the loss of mass as an important drawback of level set method. Nevertheless, they also proposed different methods to deal with this issue, for example the reinitialization of field c which may improve mass conservation. However, as it will be shown later a different approach is chosen in this study.

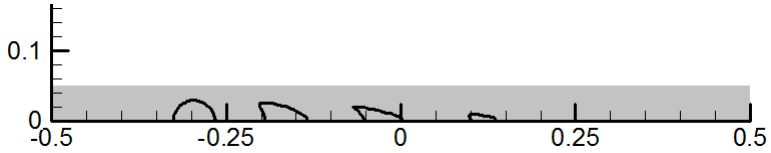

Figure 5. Evolution of a drop through a 100μm inner diameter and 1mm length straight capillary

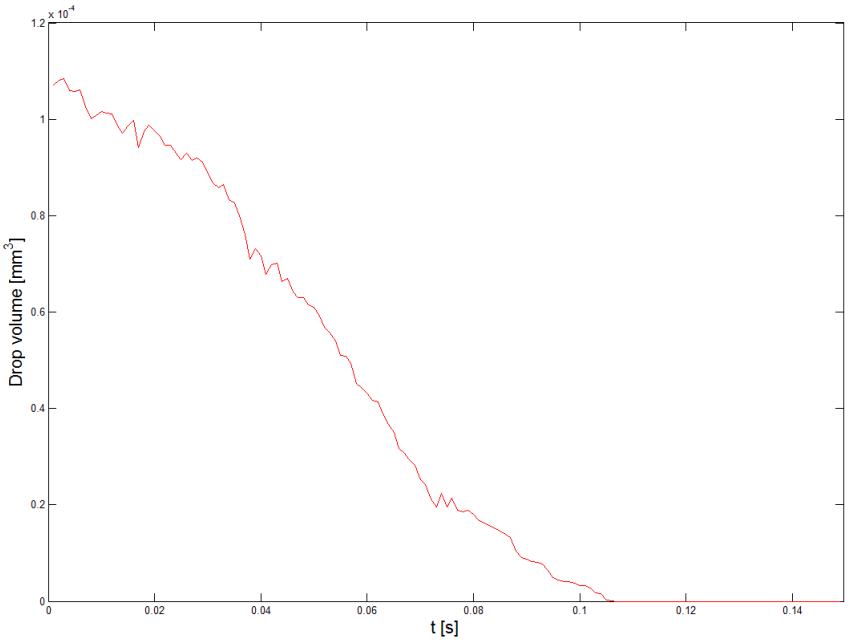

Figure 6. Drop volume versus time

In Fig. 7 the same parameters for different flow rates are considered. It is observed that there is a strong dependence between flow rate and curve slope for each case. Notice that, the smaller flow rate the softer curve slope. Hence it is important to care about how the drop moves in the grid, a fast change of its position in every time step affects the mass conservation considerably. As a consequence, there is a relation between time step and element size that should be taken into consideration in order to improve the drop volume pattern. Tsai and Miksis (1994) also reported the same observations, although they used a different method.

Figure 8 illustrates the effect of time step for flow rate $Q = 0.05ml/h$. As time step decreases, the drop evolution improves significantly. In Fig. 9 is observed that for the same last time t_f drop mass conservation is enhanced (see Fig. 9(b)).

In Fig. 10 is plotted the drop volume for a given flow rate with different time steps, note that there is a time step value which gives us practically no variation in drop volume as time evolves, obviously decreasing time steps increases the number of steps and consequently time of simulation.

4.2 Constricted capillary

It was also computed the drop dynamics through a constricted capillary considering parameters such as $\Delta t = 0.001s$, $t_f = 0.05s$, input flow rate $Q = 0.03ml/h$, output pressure $P_{OUT} = 0kPa$, $\rho = 1000kg/m^3$, μ_1=0.11 Pa.s and μ_2=0.22 Pa.s.

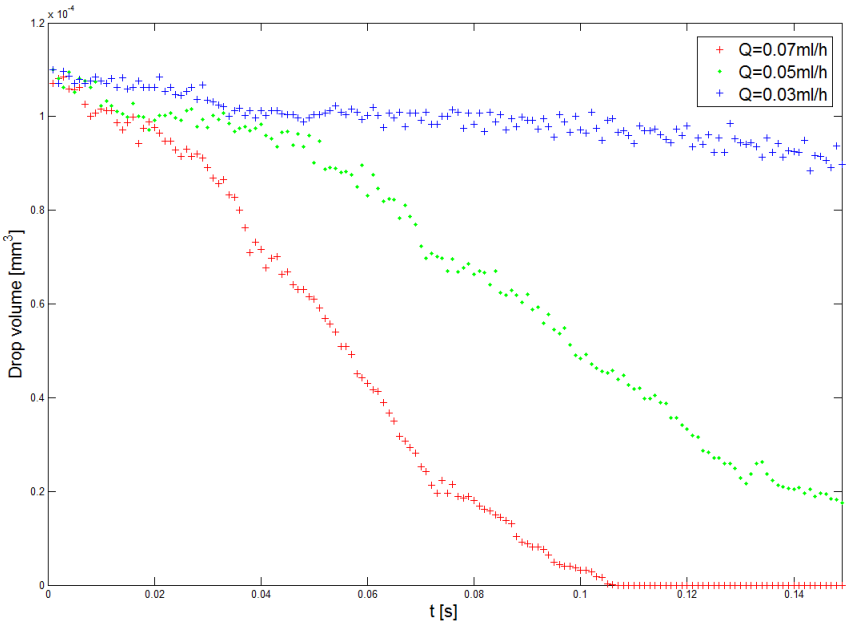

Figure 7. Drop volume evolution for three different input flow rates

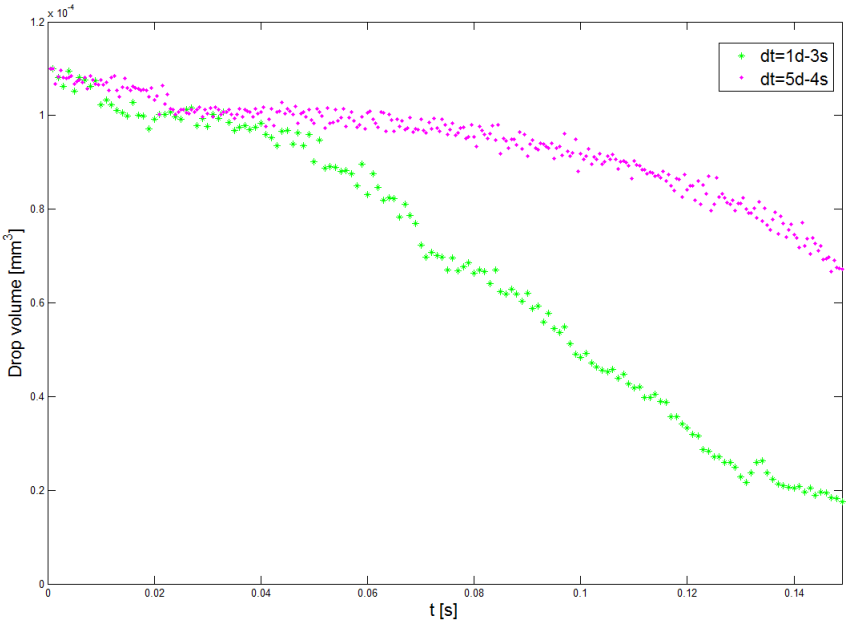

Figure 8. Drop volume evolution for $Q = 0.05ml/h$

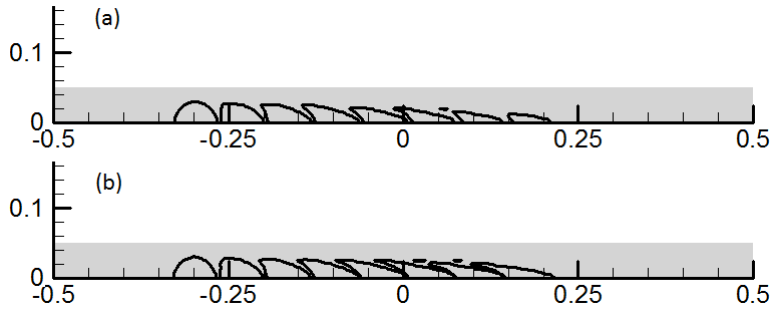

Figure 9. Drop evolution for $Q = 0.05ml/h$ and different time steps:(a) $\Delta t = 1d^{-3}s$; (b)$\Delta t = 5d^{-4}s$

Figure 11 illustrates how drop moves, it should be pointed out that is practically preserving mass.

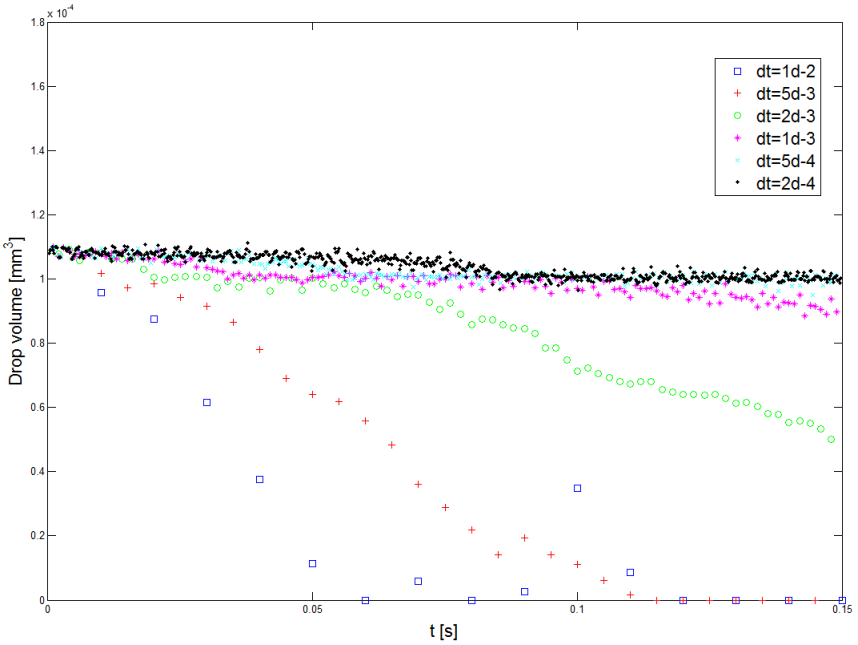

Figure 10. Drop volume for a given flow rate with different time steps

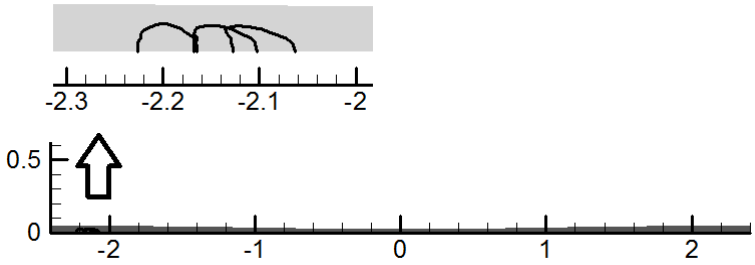

Figure 11. Drop evolution for $Q = 0.03ml/h$ through a $100/50\mu$m constricted capillary

5. CONCLUSIONS

The motion of a drop through constricted and straight capillaries has been studied. The solution were obtained by solving Navier-Stokes and level set equations with finite element method mixing Galerkin and SUPG formulations.

The pressure gradient in constricted capillaries is greater than pressure gradient in the straight one, which agrees with experimental data.

The loss of drop mass was attenuated by setting an appropriate time step value, which avoids the drop moves fast from one node to another in the next step of time.

At this stage, the model employed is not capable to deal with surface tension effects. Nonetheless, we are currently developing new algorithms to handle these issues.

6. ACKNOWLEDGEMENTS

J.F. Roca was supported by CAPES agency and PUC-Rio scholarship. Research was funded by PETROBRAS.

7. REFERENCES

Cobos, S., Carvalho, M.S. and Alvarado, V., 2009. "Flow of oil-water emulsions through a constricted capillary". *International Journal of Multiphase Flow*, Vol. 35, pp. 507–515.

Ho, B.P. and Leal, L.G., 1975. "The creeping motion of liquid drops through a circular tube of comparable diameter". *Journal of Fluid Mechanics*, Vol. 71, pp. 361–383.

McAuliffe, C.D., 1973. "Oil-in-water emulsions and their flow properties in porous media". *SPE-AIME, Chevron Oil Field Research Co.*

Olbricht, W.L. and Leal, L.G., 1982. "The creeping motion of liquid drops through a circular tube of comparable diameter: the effect of density differences between the fluids". *Journal of Fluid Mechanics*, Vol. 115, pp. 187–216.

Osher, S. and Sethian, J.A., 1988. "Fronts propagating with curvature dependent speed: Algorithm based on hamilton-jacobi formulations". *Journal of Computational Physics*, Vol. 79, pp. 12–49.

Robles, O. and Carvalho, M.S., 2010. "Oil-in-water emulsions flow through constricted micro-capillaries". *Proceedings of the 13th Brazilian Congress of Thermal Sciences and Engineering*.

Shen, E.I. and Udell, K.S., 1985. "A finite element study of low reynolds number two-phase flow in cylindrical tubes". *Journal of Applied Mathematics*, Vol. 52, pp. 253–256.

Shepel, S.V. and Smith, B.L., 2008. "On surface tension modelling using the level set method". *Intenational Journal for Numerical Methods in Fluids*, Vol. 59, pp. 147–171.

Sussman, M., Fatemi, E., Smereka, P. and Osher, S., 1995. "A level set approach for computing solutions to incompressible two-phase flow 2". *Proceedings of the 6th International Symposium on Computional Fluid Dynamics*.

Sussman, M., 1994. *A Level Set Approach for Computing Solutions to Incompressible Two-Phase Flow*. Ph.D. thesis, Department of Mathematics, University of California, Los Angeles.

Tryggvason, G., Bunner, B., Esmaeeli, A., Juric, D., Al-Rawahi, N., tauber, W., Han, J., Nas, S. and Jan, Y.J., 2001. "A front-tracking method for the computations of multiphase flow". *Journal of Computational Physics*, Vol. 169, pp. 708–759.

Tsai, T.M. and Miksis, M.J., 1994. "Dynamics fo a drop in a constricted capillary tube". *Journal of Fluid Mechanics*, Vol. 274, pp. 197–217.

8. Responsibility notice

The authors are the only responsible for the printed material included in this paper.